

## Deexcitation of He Rydberg $S$ and manifold states by $N_2$

Akira Hitachi\* and Terence A. King

*Physics Department, Schuster Laboratory, University of Manchester, Manchester M13 9PL, England*

Shinzou Kubota

*Department of Physics, Rikkyo University, Nishi-Ikebukuro, Tokyo 171, Japan*

Tadayoshi Doke

*Science and Engineering Research Laboratory, Waseda University, Shinjuku-ku, Tokyo 162, Japan*

(Received 3 March 1980)

The quenching cross sections for the He  $2S-9S$ ,  $3^1P$ , and  $n = 5-9$  manifold states by  $N_2$ , and  $n = 6-9$  manifold states by He, Ar, and Kr have been measured at 600 K. The cross section for  $2^3S$  by  $N_2$  is  $7.9(+1.2, -0.7) \text{ \AA}^2$ , and the values obtained for  $nS-N_2$  ( $n \geq 3$ ) are  $40-80 \text{ \AA}^2$  and increase slowly with  $n$  up to  $n = 5$  then show a plateau or decrease slightly with  $n$ . The cross sections for the  $^1S$  are about 1.3 times those for the  $^3S$  for  $n = 3$  and 5. The cross sections for the  $n = 5, 8,$  and  $9$  manifold states by  $N_2$  are nearly the same in magnitude as those for  $S$  states; however, those for rare-gas collisions are about one order smaller than those for  $N_2$  collisions. The main mechanism for the quenching of He Rydberg states ( $n \geq 3$ ) by  $N_2$  is attributed to  $n$ -changing collisions due to excitation of molecular vibrations in  $N_2$ .

### I. INTRODUCTION

Previously, we reported<sup>1</sup> deexcitation of Rydberg  $S$  states of helium by collisions with rare gases. The main quenching mechanism was attributed to Penning ionization for lower  $n$  states, and collisional angular-momentum transfer for highly excited states. We have extended the work to include  $N_2$  as a collision partner and to collisions which involve manifold states. Following Humphrey *et al.*,<sup>2</sup> we adopt the term manifold state to describe the collisionally mixed states, since at the helium pressures used in the present experiment higher  $l$  states are mixed with each other and we observe the decay of the mixture of these states.

When the collision partners are rare gases, the Rydberg states will be removed by angular-momentum transfer and the cross section will depend on  $l$ , mainly due to an energy spread  $\Delta E$  between  $nl$  and  $nl'$  ( $l \neq l'$ ) states. On the other hand, when the collision partners include molecules, due to energetically accessible internal degrees of freedom of molecular vibration and rotation, a different quenching process, i.e., the  $n$ -changing process, will take place. The cross section for the  $n$ -changing process should not strongly depend on  $l$ , unless strong resonance effects occur.

The quenching of Rydberg states by molecules has been studied experimentally by Czajkowski *et al.*,<sup>3</sup> Humphrey *et al.*,<sup>2</sup> and others for Na- $N_2$  collisions. However, the results of Czajkowski *et al.* and Humphrey *et al.* disagree with each other. The results obtained by Czajkowski *et al.* show resonance properties with respect to up-

ward vibrational transitions in  $N_2$  while those reported by Humphrey *et al.* do not. Bauer *et al.*<sup>4</sup> have developed a theoretical quenching model characterized by multiple potential energy curve crossings from the initial to the final states through an intermediate ionic state; the model explains reasonably well the results for Na( $nS$ )- $N_2$  collisions obtained by Humphrey *et al.* However, their results obtained for the manifold ( $l \geq 2$ ) states show a steady decrease in cross section with  $n$ , which disagrees with both the curve-crossing model and the results of Czajkowski *et al.* They explained the decrease as trapping in the manifold states.

When an atom is highly excited the valence electron is far from the ionic core and the atom appears hydrogenic. Then one can expect to be able to compare results for He- $N_2$  collisions with those for Na- $N_2$  collisions. Quenching cross sections for He Rydberg states in collision with  $N_2$  and rare gases are presented here.

### II. EXPERIMENTAL METHOD AND RESULT

The experimental method is the same as that described in Ref. 1 and is only briefly described here. The helium atoms were excited by electron impact and emissions from  $nS \rightarrow 2P$  and  $nD \rightarrow 2P$  transitions ( $n \geq 3$ ) were monitored to obtain the decay rates for the  $nS$  states and the manifold states. The emission is time resolved by single photon counting techniques. The electron beam is produced by an electron gun producing a variable duration and rapid time cut-off source. The energy of the electrons is controlled to be as close as possible to the energy of the level concerned.

The emissions from the gas cell pass through a sapphire window and a quartz lens, enter a monochromator and then photons are detected by a photomultiplier. The time difference between the pulse cut-off time and photon arrival at the photomultiplier is measured. Typical decay curves are shown in Fig. 1.

The ultimate vacuum obtained was about  $5 \times 10^{-9}$  Torr and the outgassing rate was less than  $2 \times 10^{-5}$  Torr per hour. The pressure of the gas was measured with a Baratron pressure gauge. The temperature of the experiment was 600 K with an estimated uncertainty of +200 to -100 K.

We obtained the quenching cross section by measuring the decay rate as a function of perturbing-gas pressure. The pressure dependences of some of the decay rates are shown in Figs. 2, 3, and 4.

The decay rate  $1/\tau$  for an excited state is

$$1/\tau = 1/\tau_0 + \sigma v[X], \quad (1)$$

where  $1/\tau_0$  is the total radiative decay rate of the excited state for pure helium or the total decay rate at the constant helium partial pressure used in the gas mixture.  $[X]$  is the concentration of the perturber  $X$ ,  $v$  is the average collision velocity, and  $\sigma$  is the thermal-velocity-averaged

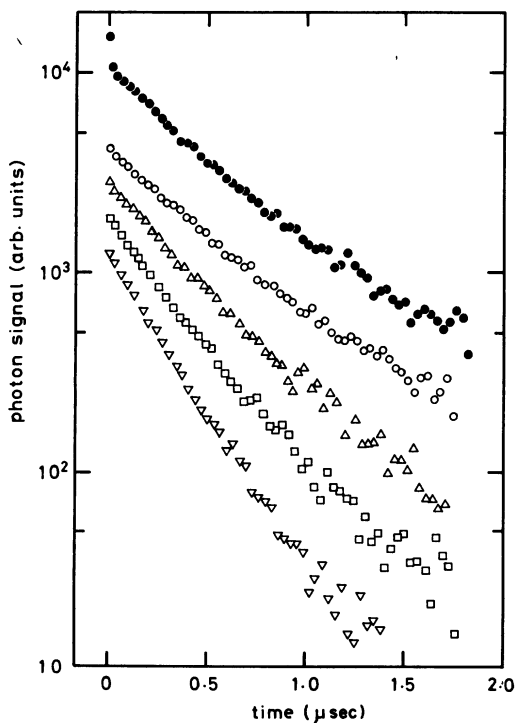


FIG. 1. Experimental decay curves for the  $8^1D$  ( $\bullet$ ) state of helium at the helium pressures of 0.5 Torr, for the  $8^3D$  state at a constant helium pressure of 0.5 Torr, and nitrogen pressures of 0 ( $\circ$ ), 41 ( $\Delta$ ), 83 ( $\square$ ), and 143 ( $\nabla$ ) mTorr.

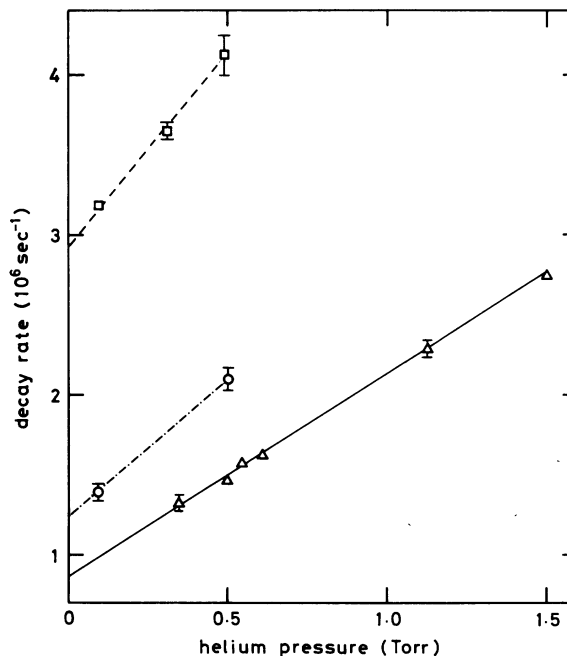


FIG. 2. Variation of decay rates for  $nD \rightarrow 2P$  emission as a function of helium pressure for  $6^3D$  ( $\square$ ),  $8^3D$  ( $\circ$ ), and  $9^3D$  ( $\Delta$ ), respectively. The decay rates correspond to those for  $l \geq 2$  manifold states as described in the text.

cross section.

The radiative decay rates of emission from  $6^3D$ ,  $8^3D$ , and  $9^3D$  are  $2.94 \pm 0.11$ ,  $1.28 \pm 0.06$ , and  $0.853 \pm 0.042$  in  $10^6 \text{ sec}^{-1}$ , respectively, and are much lower than the theoretical radiative decay rates of those states.<sup>5</sup> The decay rates obtained here are interpreted to represent the decays of  $l \geq 2$  manifold states; at the helium pressure used in the present experiment  $nD$  states are very rapidly

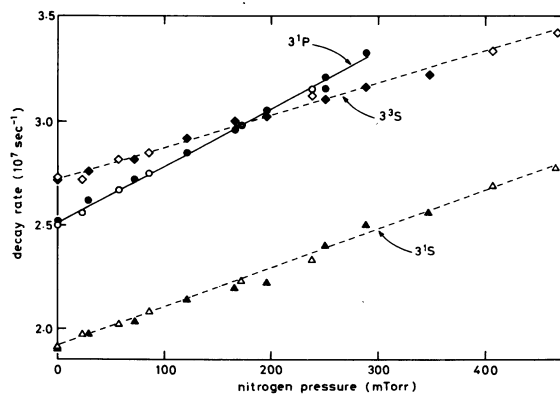


FIG. 3. Variation of decay rates for helium excited states as a function of nitrogen gas pressure at a constant helium pressure of 1 Torr for  $3^1S$  ( $\Delta$ ),  $3^3S$  ( $\diamond$ ), and  $3^1P$  ( $\circ$ ); open and closed symbols show results for different runs.

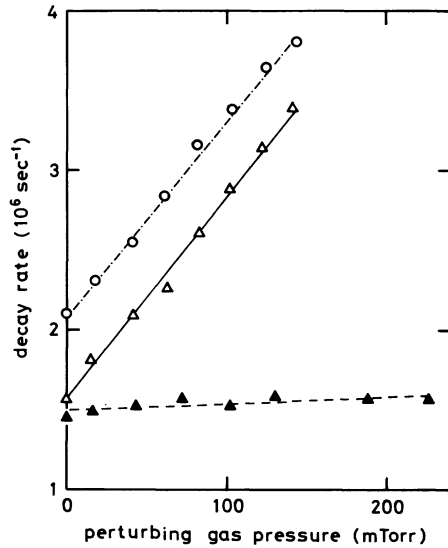


FIG. 4. Variation of decay rates for  $nD \rightarrow 2P$  emission as a function of perturbing-gas pressure at constant helium pressure for  $8^3D\text{-N}_2$  (○),  $9^3D\text{-N}_2$  (△), and  $9^3D\text{-Ar}$  (▲), and helium pressures of 0.5, 0.545, and 0.5 Torr, respectively.

mixed with the higher  $l$  states and then emissions from the  $nD$  states show the decay of the mixed states.

The decays of  $n^1D \rightarrow 2^1P$  emission showed double exponential forms. The slow decay component is similar to the decay of  $n^3D \rightarrow 2^3P$  emission as shown in Fig. 1, while the fast decay may possibly be attributed to transfer from and decay of  $n^1P$ , or to cascade from and decay of  $(n+1)^1P$  states.

Emission from the  $3^1P \rightarrow 2^1S$  transition was monitored to obtain the decay rate for the  $3^1P$  state. The decay rate for the  $n=5$  manifold state was obtained by monitoring  $3^3D \rightarrow 2^3P$  emission, the  $5^3F$  state cascades to lower  $n^3D$  states, and one can observe the decay rate corresponding to the  $n=5$  manifold state in emission from the  $3^3D$  state.

A cross section of  $7.9(+1.2, -0.7) \text{ \AA}^2$  is obtained

for the quenching of the  $2^3S$  metastable state by  $\text{N}_2$  collisions by monitoring the nitrogen first negative system. Details of the quenching of the metastable atoms will be published elsewhere.

The cross sections obtained for  $\text{He}(nS)\text{-N}_2$  collisions increase with  $n$  up to  $n=5$  and then show a plateau or decrease slightly with  $n$  as shown in Table I and Fig. 5. The main contribution to the errors given in Table I are systematic errors of  $(+15, -8)\%$  due to the uncertainty in the determination of the gas temperature; for  $8^3S\text{-N}_2$  and  $9^3S\text{-N}_2$  the measurement error is larger. The systematic errors are not included in the error bars shown in Fig. 5. The cross sections obtained for the singlet states are about 1.3 times those for the triplet states for  $n=3$  and 5.

### III. DISCUSSION

The cross sections measured for  $\text{N}_2$  quenching of the  $n=5, 8,$  and  $9$  manifold states are almost the same in magnitude as those for  $S$  states; this result disagrees with that obtained by Humphrey *et al.* for  $\text{Na-N}_2$  collisions for which the cross sections for manifold states were less than half of those for  $S$  states at the same  $n$ . The main mechanism for the quenching of helium Rydberg states by  $\text{N}_2$  is attributed to  $n$ -changing collisions due to an energetically accessible internal degree of freedom of  $\text{N}_2$  molecular vibrations; this does not apply to the  $2^3S$  metastable state for which Penning ionization is responsible for the quenching.

We estimate the  $n$ -changing quenching cross sections by the curve-crossing model developed by Bauer *et al.* and simplified by Humphrey *et al.* The model is characterized by multiple energy curve crossings from the initial to the final states through an intermediate ionic state. The approximate ionic  $\text{He}^+\text{-N}_2^-$  curve and the excited  $\text{He-N}_2$  interaction potentials are shown in Fig. 6 as a function of internuclear separation  $r$ . Although there are curves corresponding to the excited vibrational states of  $\text{N}_2$  and  $\text{N}_2^-$  above the curves of Fig. 6, we have omitted these for clarity.

TABLE I. Cross sections for the quenching of He Rydberg states by He and  $\text{N}_2$  measured at  $600(+200, -100)$  K.  $^3S(\text{calc})$  is the cross section for the  $n$ -changing process calculated by Eq. (2). All cross sections are in  $\text{\AA}^2$ .

$n$	$^1P$	$^1S$	$^3S$	$^3S(\text{calc})$	Manifold state	
	He- $\text{N}_2$	He- $\text{N}_2$	He- $\text{N}_2$	He- $\text{N}_2$	He- $\text{N}_2$	He-He
2			$7.9(+1.2, -0.7)$			
3	$88.3(+13.3, -7.2)$	$62.0(+9.6, -5.5)$	$49.9(+7.6, -4.2)$	45		
4		$71.5(+11.3, -6.6)$		79		
5		$76.4(+12.1, -7.2)$	$58.3(+9.4, -5.7)$	102	$66.8(+12.2, -8.6)$	
6				121		$5.7(+1.3, -1.1)$
8			$42(+16, -9)$	145	$40.3(+6.6, -4.1)$	$4.3(+0.8, -0.6)$
9			$48(+14, -9)$	153	$41.1(+6.5, -3.9)$	$3.1(+0.5, -0.3)$

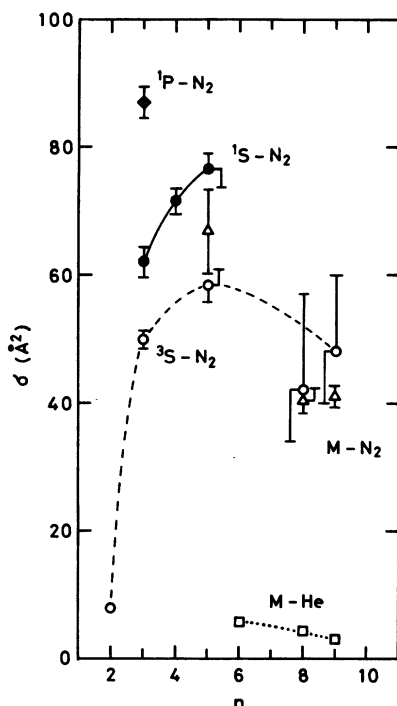


FIG. 5. Quenching cross sections measured for helium Rydberg states by collisions with He and  $N_2$ ;  $3^1P-N_2$  ( $\blacklozenge$ ),  $n^1S-N_2$  ( $\bullet$ ),  $n^3S-N_2$  ( $\circ$ ), manifold state  $N_2$  ( $\Delta$ ), and manifold state He ( $\square$ ). The error bars do not include systematic errors of  $(\pm 15, -8)\%$  due to the uncertainty in the determination of the atom temperature.

A specified initial state  $He(nl) + N_2(X^1\Sigma_g^+, v=0)$ , after passing through many curve crossings, goes to  $He(n'l') + N_2(X^1\Sigma_g^+, v')$  states which are energetically accessible. Then, the quenching cross section is approximately given by

$$\sigma = \pi r_c^2, \quad (2)$$

where  $r_c$  is the radius of the outermost curve crossing. The ionic potential curves are given by a Coulomb-plus-polarizability interaction

$$V(r) = E_\infty - (e^2/r) - (e^2\alpha/2r^4), \quad (3)$$

where  $e$  is the electronic charge,  $\alpha$  is the sum of the polarizability of the  $He^+$  and  $N_2^-$  pair, and  $E_\infty$  is the difference between the ionization potential of He and the electron affinity of  $N_2$ . For the electron affinity of  $N_2$  we use the value of  $-1.89$  eV (Ref. 6). No value is available for the polarizability, but, since the polarizability interaction term becomes very small for large  $r$ , we can omit the polarizability term for large  $n$ . If one chooses a very large polarizability, for example,  $\alpha = 100 \text{ \AA}^3$ , one will obtain for  $n=3$  twice the cross section value compared with the choice of zero polarizability correction and 1.2 times for  $n=10$ . We have assumed also that the excited interaction

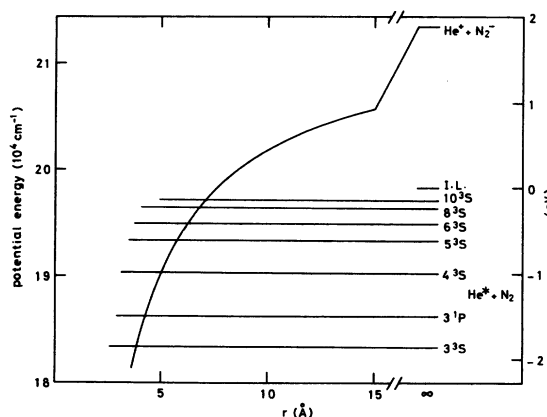


FIG. 6. Potential-energy curves for  $He+N_2$  system which show the covalent  $He-N_2$ ,  $v=0$  curve, and the ionic  $He^+-N_2^-$ ,  $v=0$  curve.

potentials are equal to those at  $r = \infty$  for  $r$  greater than  $r_c$ . The values obtained in this way for  $n^3S$  are shown in Table I together with experimental values.

As shown in the table, the model gives cross sections of the same order of magnitude as the present experimental results and which also increase slowly with  $n$ . Present experimental results give the same trend up to  $n=5$  but do not show an increase in the cross section for higher  $n$ . The reason why the cross sections do not increase with  $n$  for higher  $n$  probably results because, for higher  $n$  states, the electron density of the atom decreases with  $n$  and then the probability of finding the Rydberg electron when the  $N_2$  molecule comes near to the He nucleus decreases. The curve-crossing model also predicts nearly the same value for the S and manifold states and this agrees with present results.

The angular-momentum transfer cross sections calculated by a semiclassical model<sup>1</sup> proposed by Gersten,<sup>7</sup> in which the interaction between the highly excited atom and the perturber is approximated by a Breit-Fermi pseudopotential, are 9 and  $14 \text{ \AA}^2$  for  $8^3S-N_2$  and  $9^3S-N_2$ , respectively, and are much smaller than the values obtained here. The electron scattering length used<sup>8</sup> in these calculations was  $0.7 a_0$ .

The cross sections obtained for the quenching of the manifold states by rare gases are very small. Those for He collisions decrease with  $n$  as shown in Table I and Figs. 2 and 5. The cross section for the  $6^3D$  manifold state by Kr is  $5.7(+1.5, -1.3) \text{ \AA}^2$ ; that for the  $9^3D$  manifold state by Ar is  $1.4(+0.8, -0.7) \text{ \AA}^2$ , and those for  $7^3D$  and  $8^1D$  manifold states by Ar are less than  $2 \text{ \AA}^2$ . The quenching mechanism for the manifold states by rare gases is expected to be due to  $n$ -changing collisions.

ions and Penning ionization, and both cross sections will be small for the values  $n$  of concern here.

Devos *et al.*<sup>9</sup> have measured the collisional depopulation rates for He Rydberg states by He using time-resolved laser induced spectroscopy and reported that the rates are nearly independent of  $n$  for  $8 \leq n \leq 17$ . The cross sections for  $n=8$  and 9 are about 15 and 14 Å<sup>2</sup>, respectively, assuming Maxwellian average velocity at  $T=300$  K. Present results are less than those obtained by Devos *et al.* which were much larger than the values predicted by Flannery's<sup>10</sup> semiclassical binary-encounter theory.

Quite recently, Janev and Mihajlov<sup>11</sup> have proposed the quasideviant energy transfer model. The main idea of the mechanism lies in considering the transitions of the Rydberg electron as being resonantly coupled with the transitions in the quasimolecular subsystem of the perturbing atom and the ionic core of the Rydberg atom. They calculated the velocity dependence of the  $n$ -changing process of H( $n$ )-H collisions for  $n=10$  to 14. The magnitude of the cross sections for  $v \leq 10^6$  cm/sec is of the order of 1 to 10 Å<sup>2</sup> and decreases with an  $n$  increase.

If one estimates the cross section for He-He collisions from the values obtained for H-H collisions and only taking into account the velocity change, one obtains cross sections somewhat larger than the present results. However, this may overestimate the cross section; Janev and Mihajlov suggested that a large binding energy

gives a small cross section. The collision energy may not be high enough, compared with the internal energy changes, to apply the model to the thermal collisions of the  $n$  values of concern here. The reason why the singlet states are more strongly quenched by nitrogen than the triplet states is not understood at present.

The relatively large value obtained for the  $3^1P$  resonance state may be due to a contribution from Penning ionization. The cross section for the ionization process due to the optically allowed transition  $A^* + X \rightarrow A + X^+ + e^-$  has been studied by Watanabe and Katsuura<sup>12</sup> and is given by

$$\sigma = 13.9(\mu^2 \mu_B^2 / \hbar v)^{2/5}, \quad (4)$$

where  $\mu$  and  $\mu_B$  are the transition dipole moment associated with the transition  $A \rightarrow A^*$  and  $X \rightarrow X^+ + e^-$ , respectively. We calculate for the thermal velocity-averaged cross section for He( $3^1P$ )-N<sub>2</sub> collisions a value of 33 Å<sup>2</sup>. We used  $\mu^2 = 0.0433$  a.u. (Ref. 13) and the value of  $\mu_B$  was deduced from experimental photoionization cross section.<sup>14</sup> Then the contribution from the  $n$ -changing process will be about 55 Å<sup>2</sup> which agrees well with the calculated values of 55 Å<sup>2</sup> from Eq. (2).

#### ACKNOWLEDGMENTS

We would like to acknowledge many helpful discussions with Dr. M. Matsuzawa and we thank Dr. H. J. Baker for his help with the electronics. Partial funding for this study has been provided by the U. K. Science Research Council.

\*On leave from Science and Engineering Research Laboratory, Waseda University, Shinjuku-ku, Tokyo 162, Japan.

<sup>1</sup>A. Hitachi, T. Doke, S. Kubota, and T. A. King, *At. Col. Res. Jpn.* **4**, 97 (1978); A. Hitachi, T. Doke, S. Kubota, C. Davies, and T. A. King, in *Abstracts of the Eleventh International Conference on the Physics of Electronic and Atomic Collisions, Kyoto, 1979* (The Society for Atomic Collision Research, Kyoto, 1979).

<sup>2</sup>L. M. Humphrey, T. F. Gallagher, W. E. Cooke, and S. A. Edelstein, *Phys. Rev. A* **18**, 1383 (1978).

<sup>3</sup>M. Czajkowski, L. Krause, and G. M. Skardis, *Can. J. Phys.* **51**, 1582 (1973).

<sup>4</sup>E. Bauer, E. R. Fisher, and F. R. Gilmore, *J. Chem. Phys.* **51**, 4173 (1969).

<sup>5</sup>A. H. Gabriel and D. W. O. Heddle, *Proc. R. Soc. London Ser. A* **258**, 124 (1960).

<sup>6</sup>J. C. Y. Chen, *J. Chem. Phys.* **40**, 3513 (1964). Here we assume N<sub>2</sub> is spherically symmetric.

<sup>7</sup>J. I. Gersten, *Phys. Rev. A* **14**, 1354 (1976).

<sup>8</sup>C. Fuchtbauer, P. Schulz, and A. F. Brandt, *Z. Phys.* **90**, 403 (1934).

<sup>9</sup>F. Devos, J. Boulmer, and J.-F. Delpéch, *J. Phys. (Paris)* **40**, 215 (1979).

<sup>10</sup>M. R. Flannery, *Ann. Phys. (N.Y.)* **61**, 465 (1970).

<sup>11</sup>R. K. Janev and A. A. Mihajlov, *Phys. Rev. A* **20**, 1890 (1979).

<sup>12</sup>T. Watanabe and K. Katsuura, *J. Chem. Phys.* **47**, 800 (1967).

<sup>13</sup>W. L. Wiese, M. W. Smith, and B. M. Glennon, *Atomic Transition Probabilities*, U. S. Natl. Bur. Stand., National Standard Reference Data Series-4 (U.S. G.P.O., Washington D. C., 1966), Vol. 1.

<sup>14</sup>G. R. Cooke and P. H. Metzger, *J. Chem. Phys.* **41**, 321 (1964). Since the photoionization cross section of nitrogen at 53.7 nm (corresponding to the helium  $3^1P \rightarrow ^1S_0$  transition) is not available, the value at 60 nm was used.